

Modification of polyvinylidene fluoride and polysulfone flat sheet membranes using perovskite nanoparticles for treatment of humic acid in a submerged membrane system

Abolfazl Sadeghiazar Sharabiani^a, Seyed Jamaledin Peighambaroust^{a,*}, Aligholi Niaei^a, Parisa Mohammadzadeh Pakdel^a, Yilmaz Yildirim^b, Ali Kemal Topaloglu^b

^aFaculty of Chemical and Petroleum Engineering, University of Tabriz, Tabriz 5166616471, Iran, emails: j.peighambaroust@tabrizu.ac.ir (S.J. Peighambaroust), sadeghiabolfazl75@gmail.com (A.S. Sharabiani), aniaei@tabrizu.ac.ir (A. Niaei), parisa.mohammadzadeh90@gmail.com (P.M. Pakdel)

^bDepartment of Environmental Engineering, University of Bulent Ecevit, Zonguldak, Turkey, emails: yilmaz.yildirim@beun.deu.tr (Y. Yildirim), alikemal.topaloglu@beun.deu.tr (A.K. Topaloglu)

Received 13 October 2022; Accepted 3 May 2023

ABSTRACT

In this work, the effects of incorporating perovskite nanoparticles into polyvinylidene fluoride (PVDF) and polysulfone (PS) flat sheet membranes were evaluated in detail. perovskite nanoparticles were added in a low amount (1 wt.%) to the casting solution to fabricate nanocomposite membranes with the non-solvent induced phase separation method. Prepared membranes were characterized using atomic force microscopy (AFM), scanning electron microscopy-energy-dispersive X-ray spectroscopy, and contact angle techniques. AFM images demonstrated that perovskite-embedded membranes had smoother surfaces than neat PVDF and PS membranes. Contact angle measurement showed that the hydrophilicity of PVDF and PS membranes was improved by adding nanoparticles. Results revealed that the presence of perovskite nanoparticles in the matrix of the membrane improves pure water flux from 58.0 (neat PVDF) and 44.9 (neat PS) to 66.1, 71.8, 56.3, and 64.5 L/m²·h for PVDF/LaSrCuMn, PVDF/LaSrCuMn-Pd, PS/LaFeMn, and PS/LaFeMn-Pd nanocomposite membranes, respectively. The fouling behavior of prepared membranes was ascertained by filtration of humic acid solution. Investigation of antifouling performance showed that nanocomposite membranes have higher fouling resistance. Finally, it was found that nanocomposite membranes can be used efficiently to filter humic acid.

Keywords: Perovskite nanoparticles; Membrane fouling; Polyvinylidene fluoride; Polysulfone

1. Introduction

The need for healthy water is rising due to the rapid growth of the world population. It was estimated that one billion people don't have access to drinking water, and five million die from being forced to use unhealthy water [1]. Various decontamination methods, such as adsorption [2], ion exchange [3], coagulation [4], and membrane

separation [5], are used to remove water pollutants. Among them, membrane separation is an effective method due to low energy consumption, easy scale-up, less or no use of chemicals, low maintenance cost, and absence of any harmful byproduct formation. One of the main drawbacks of membrane application in water treatment is fouling, leading to a decrement in the permeability and lifetime of the membrane. The natural organic materials in surface water

* Corresponding author.

are the main cause of membrane fouling in the ultrafiltration process. Humic acid (HA) is one of the organic substances of surface waters that produce from the degradation of carbohydrates, lignin, and high molecular weight protein [6]. It gives color to water when its concentration exceeds 5 mg/L and reacts with heavy metal-producing metal complexes [7]. Also, it reacts with other substances and produces toxic contaminants in water resources [8]. Organic polymers and inorganic materials like ceramic can fabricate membranes, but ceramic membranes are brittle and expensive [9]. Therefore, various polymers such as polyethylene (PE), polyvinyl chloride (PVC) [10], polypropylene (PP) [11], polysulfone (PS) [12], and polyvinylidene fluoride (PVDF) [13] are used to develop polymeric membranes. Due to low cost and high mechanical, thermal, and chemical stability, PS and PVDF are popular polymers used to produce microfiltration (MF) and ultrafiltration (UF) membranes. Besides these advantages, their membranes lack hydrophilicity, the absence of active functional groups, and non-wettability. This leads to being fouled by colloids and organics during the filtration process [14]. Membrane foulants are divided into three groups, including inorganic, organic, and biofouling which causes internal blocking or external deposition on the membrane surface [15]. Membrane fouling increases operational costs and decrement in pure water flux and membrane lifetime [16]. Different approaches are used to solve this problem, such as polymer blending, nanoparticle embedding, and chemical grafting. Various nanoparticles such as clays [17], halloysite [18], SiO₂ [19], graphene oxide [16], and reduced graphene oxide [20] are incorporated into the membrane matrix, which enhances membrane fouling resistance and hydrophilicity. Two-dimensional (2D) materials can improve the selective performance of polymeric membranes by acting as a shield in their structure. For example, boron nitride (BN) has gained a special place in modifying polymeric membranes due to showing excellent strength in acidic and inorganic environments, high surface area, and thermal stability. Vatanpour et al. [21] fabricated polyethersulfone (PES) mixed matrix membranes embedded with different amounts of amine-functionalized boron nitride (AFBN). The obtained results showed that the modified membrane with 1 wt.% (AFBN) have the highest amount of Reactive Blue 19 rejection (99.7%) and the least degree of fouling (90.4%). Another modification method is coating an ultrathin layer on a porous membrane. Mansourpanah et al. [22] modified PES membranes' properties by forming a thin chitosan layer and used microwave radiation to graft acrylamide onto the chitosan backbone. The effect of acrylamide concentration, irradiation time, and power was studied using the Taguchi method. In some studies, various metal oxides, such as TiO₂ [11], ZnO [23], CuO [23], and Al₂O₃ [13], are used to improve hydrophilicity and mitigate membrane fouling. These nanoparticles can be integrated into membrane structure by blending with polymeric matrix or surface deposition and alter intrinsic properties of membranes such as porosity by increasing precipitation rate. During the last decades, perovskite oxides, with the general formula ABO₃ or A₂BO₄, have been a fundamental class of functional materials that exhibit a range of stoichiometries and crystal structures. These materials have

gained various industrial applications in catalysis, fuel cells, sensors, gas-separable membranes, and electrolytes. Because of the structural features, they could accommodate around 90% of the natural metallic elements of the periodic table that stand solely or partially at the A and/or B positions without destroying the matrix structure, offering a way of correlating solid-state chemistry to catalytic properties. Moreover, their high thermal and hydrothermal stability makes them suitable catalytic materials for gas or solid reactions at high or liquid reactions at low temperatures [24,25]. The sol–gel method is an effective way to synthesize these nanoparticles with high dispersity. To the author's knowledge, no studies have been performed on using perovskite oxide nanoparticles in the polymeric matrix of membranes.

In the current study, PS and PVDF ultrafiltration membranes were fabricated by the non-solvent induced phase separation (NIPS) method to remove HA from contaminated water. Polyvinylpyrrolidone (PVP) was used as a pore-forming agent to enhance pure water flux. To improve the fouling properties of fabricated membranes, LaSrCuMn, LaFeMn, LaSrCuMn-Pd, and LaFeMn-Pd perovskite oxide nanoparticles were incorporated into the matrix of the membrane. The morphology, wettability, water flux, fouling behavior, and rejection abilities of fabricated membranes were investigated in detail.

2. Experimental set-up

2.1. Material

N-methyl-2-pyrrolidone (NMP), polysulfone (PS, $M_w = 22,000$ Da), polyvinylidene fluoride (PVDF, $M_w = 534,000$ Da), polyvinylpyrrolidone (PVP, $M_w = 10,000$ Da), citric acid monohydrate, and humic acid (HA) were purchased from Sigma-Aldrich Co., (Gillingham, United Kingdom) La(NO₃)₃·6H₂O, Cu(NO₃)₂·3H₂O, Pd(NO₃)₂·2H₂O, Mn(NO₃)₂·4H₂O, Fe(NO₃)₃·9H₂O, and Sr(NO₃)₂·4H₂O were purchased from Merck (Darmstadt, Germany).

2.2. Characterizations

The morphology of membranes was demonstrated by scanning electron microscopy (SEM-TESCAN MIRA3-FEG) coupled with an energy-dispersive X-ray spectroscopy (EDAX). After fracturing in liquid nitrogen, the surface of the samples was made conductive with gold by sputtering. The surface roughness of fabricated membranes was investigated using atomic force microscopy (AFM; Microscope NANOSURF Mobile S). Contact angles of the membrane top surface were measured three times at different positions on each sample by a contact angle meter (CAG-20SE, JIKAN, Tehran).

2.3. Synthesis of perovskites

A sol–gel synthesis approach using the metal nitrate precursor materials (La(NO₃)₃·6H₂O, Cu(NO₃)₂·3H₂O, Pd(NO₃)₂·2H₂O, Mn(NO₃)₂·4H₂O, Fe(NO₃)₃·9H₂O, and Sr(NO₃)₂·4H₂O) was followed for preparation of perovskite nanoparticles. To prepare 1.0 g of nanoparticles, an appropriate amount of metal nitrates with nominal cation ratios were dissolved in 50 mL of de-ionized water. Citric acid

monohydrate is added to the solution of the cations with a molar ratio of 1:0.525 concerning the total amount of cations. Then, the solution was heated up to 80°C with stirring until a sticky gel was obtained. The gel is heated to 200°C for 2 h in the air to remove the organic ligands, decompose the nitrates, and turn them into dark powder. Final calcination for 5 h at 700°C yielded the oxidized starting materials [25].

2.4. Preparation of membranes

To prepare neat PVDF (M1), PS (M2), and PVDF/LaSrCuMn (M1-1), PS/LaFeMn (M2-1), PVDF/LaSrCuMn-Pd (M1-2) and PS/LaFeMn-Pd (M2-2) nanocomposite membranes, the NIPS technique was used. At first, 1 wt.% perovskite nanoparticles were stirred in NMP solvent (80 wt.%), then the prepared solution was sonicated in an ultrasonic bath for 30 min to better dispersion of the nanoparticles in the solvent. Afterward, PS or PVDF (18 wt.%) and PVP (1 wt.%) as pore agents were added to the prepared solution and stirred for a complete polymer solution. The ready solution was cast on a glass plate with a steel knife with a 400 μm gap and immersed in a water coagulation bath. To complete the phase inversion process, the cast film was immersed in a DI water bath for 24 h.

2.5. Membrane porosity

The gravimetric method was used to calculate the membranes' porosity (ϵ , %). The mathematical relation of the gravimetric method is represented as follows:

$$\epsilon(\%) = \frac{\frac{W_w - W_d}{D_w}}{\frac{W_w - W_d}{D_w} + \frac{W_d}{D_p}} \times 100 \quad (1)$$

where W_w , W_d , D_w , and D_p are the weight of wet (immersed in water for 24 h), dry (dried at 70°C for 8 h) membrane, and density of water (0.998 g/cm³) and polymers (1.78 g/cm³ for PVDF and 1.24 g/cm³ for PS), respectively.

2.6. Pure water flux, antifouling performance, and rejection

A submerged membrane filtration system was used to determine pure water flux. Compacting of pre-wetted membranes was performed at a pressure of 0.8 bar for 40 min to minimize compaction effects. Then, pressure is reduced to 0.5 bar to determine pure water flux. After reaching a steady state, pure water flux (J_w) was calculated as follows:

$$J_w = \frac{V}{At} \quad (2)$$

where V (L) is the volume of permeate, A (m²) is membrane surface area, and t (h) is permeation time. After determining pure water flux, to investigate the antifouling properties of prepared membranes, the flux of HA solution (JP) with a concentration of 1 g/L as an organic foulant model

was calculated every 5 min for 45 min. After filtration of HA, membranes were washed with distilled water several times to eliminate reversible fouling, and pure water flux was determined again ($J_{w,2}$). The following equation determined the flux recovery ratio (FRR):

$$\text{FRR}(\%) = \frac{J_{w,2}}{J_{w,1}} \times 100 \quad (3)$$

The reversible fouling ratio (RFR), irreversible fouling ratio (IFR), and total fouling ratio (TFR) were calculated by Eqs. (4)–(6):

$$\text{RFR}(\%) = \frac{J_{w,2} - J_p}{J_{w,1}} \times 100 \quad (4)$$

$$\text{IFR}(\%) = \frac{J_{w,1} - J_{w,2}}{J_{w,1}} \times 100 \quad (5)$$

$$\text{TFR}(\%) = \text{RFR} + \text{IFR} = \frac{J_{w,1} - J_p}{J_{w,1}} \times 100 \quad (6)$$

The following equation calculated the HA rejection of membranes (R %):

$$R(\%) = \left(1 - \frac{C_p}{C_f} \right) \times 100 \quad (7)$$

where C_f and C_p (g/L) are the concentration of HA in feed and permeate solution, respectively.

3. Results and discussion

3.1. SEM-EDAX analysis

The cross section of prepared membranes is depicted in Fig. 1a–h. As shown in Fig. 1a, the neat PVDF membrane has a fibrous-like microstructure with inter-connected pores. In contrast, the neat PS membrane has finger-like pores (Fig. 1b). As can be seen from SEM images (Fig. 1c–f), nanocomposite membranes had asymmetric structures including dense skin at the top, finger-like voids at the middle layer, which connected using spongy walls, and macrovoid at the bottom layer. The finger-like and macrovoids of nanocomposite membranes are larger than neat membranes due to the presence of perovskite nanoparticles. Adding perovskite nanoparticles affects the thermodynamics and kinetics of the phase separation process in a way that enhances the exchange rate of solvent and non-solvent [26]. A comparison of SEM images of nanocomposite membranes showed that layers are closer in nanocomposite membranes containing LaSrCuMn-Pd and LaFeMn-Pd nanoparticles. To investigate perovskite nanoparticle dispersion in the cross-section of membranes, EDAX analysis was used. Based on obtained results, peroxide nanoparticles are well distributed in the cross-section of membranes without any aggregation (Figs. 2 and 3).

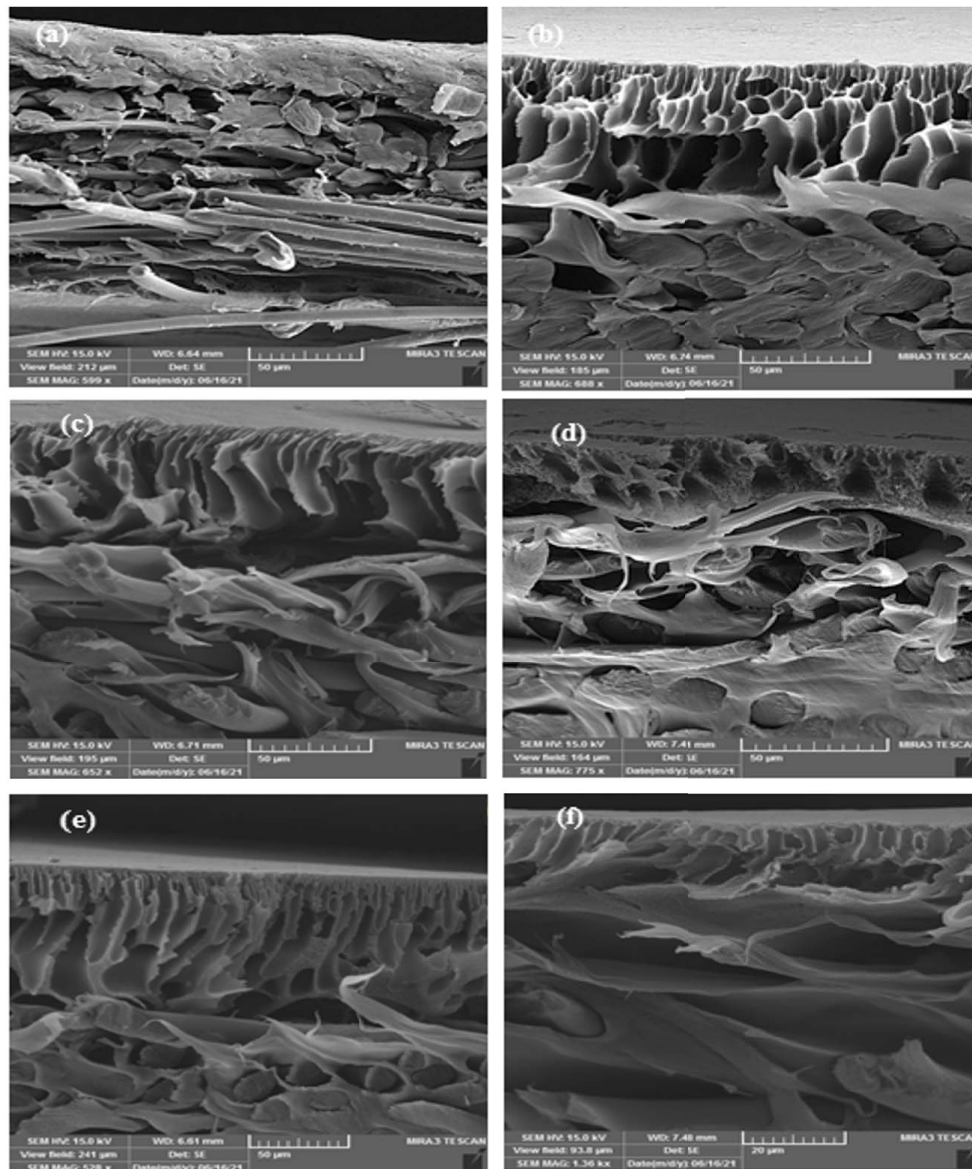


Fig. 1. Scanning electron microscopy images of (a) M1, (b) M2, (c) M1-1, (d) M2-1, (e) M1-2, and (f) M2-2.

3.2. AFM analysis

To study the surface morphology of membranes, AFM analysis was performed. Fig. 4a–f shows three-dimensional AFM images of M1, M2, M1-1, M2-1, M1-2, and M2-2 membranes which bright and dark regions are related to the highest point of the membrane surface and pores or valleys of the membrane, respectively. The roughness parameters of prepared membranes (S_a , mean roughness; S_r , root-mean-square of Z data; and S_v , the height difference between the highest peak and the lowest valley) are presented in Table 1. Mean roughness of the neat PVDF membrane is higher than the neat PS membrane. In both membranes, the addition of perovskite nanoparticles decreases the mean roughness. Also, the presence of Pd-treated perovskite nanoparticles enhances mean roughness compared to perovskite-containing membranes. According to reported studies, membranes

with higher roughness possess lower antifouling ability due to the accumulation of pollutants on the surface valleys of membranes [27].

3.3. Contact angle and porosity

To evaluate the hydrophilicity of the surface of the membrane, the contact angle should be measured, which provides valuable information about the solid–liquid interfacial energy [28]. Hydrophilicity has a crucial effect on the flux and antifouling properties of the membranes [7]. The contact angle of neat and nanocomposite membranes is illustrated in Fig. 5a. The results show that the contact angle of nanocomposite membranes is smaller than neat ones, so nanocomposite membranes are more hydrophilic than PS and PVDF membranes. It can be ascribed to the presence of hydrophilic nanoparticles in the structure of

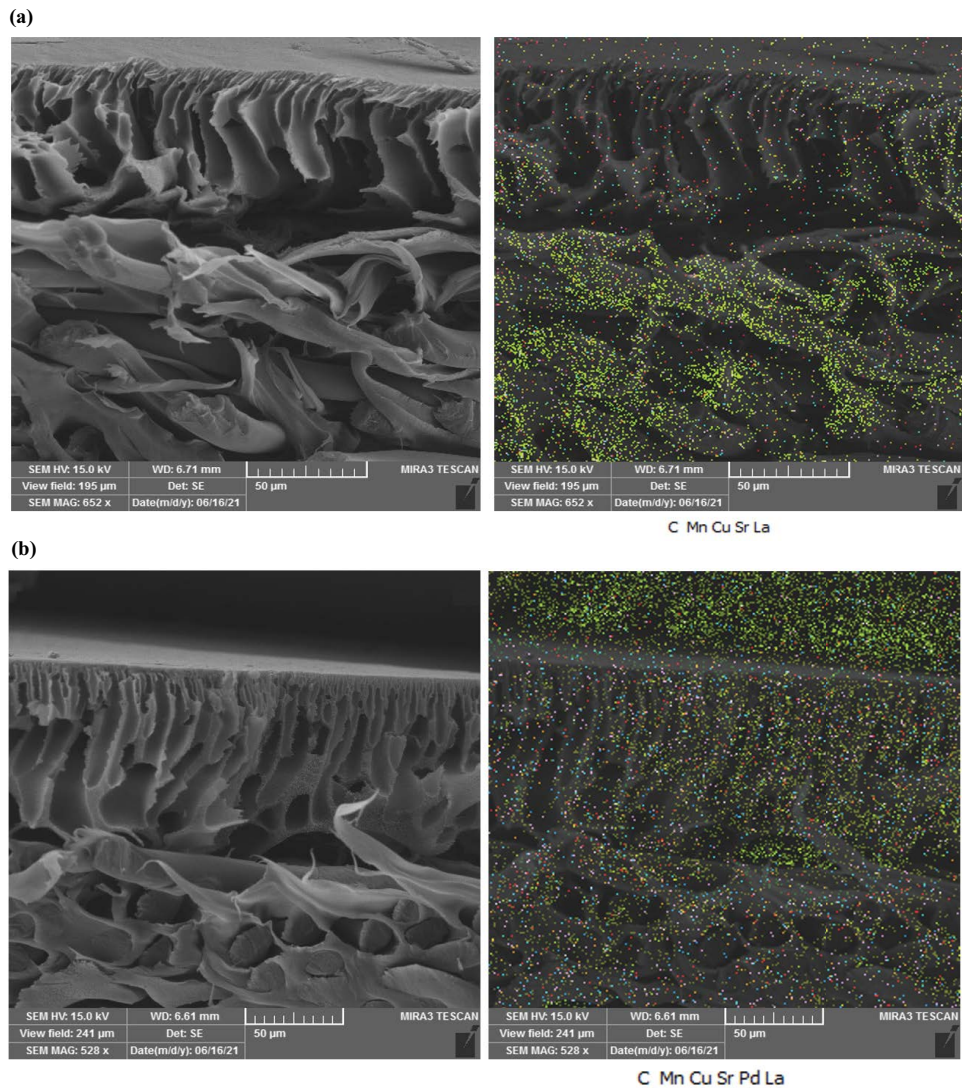


Fig. 2. Energy-dispersive X-ray spectroscopy-mapping of (a) M1-1 and (b) M2-1.

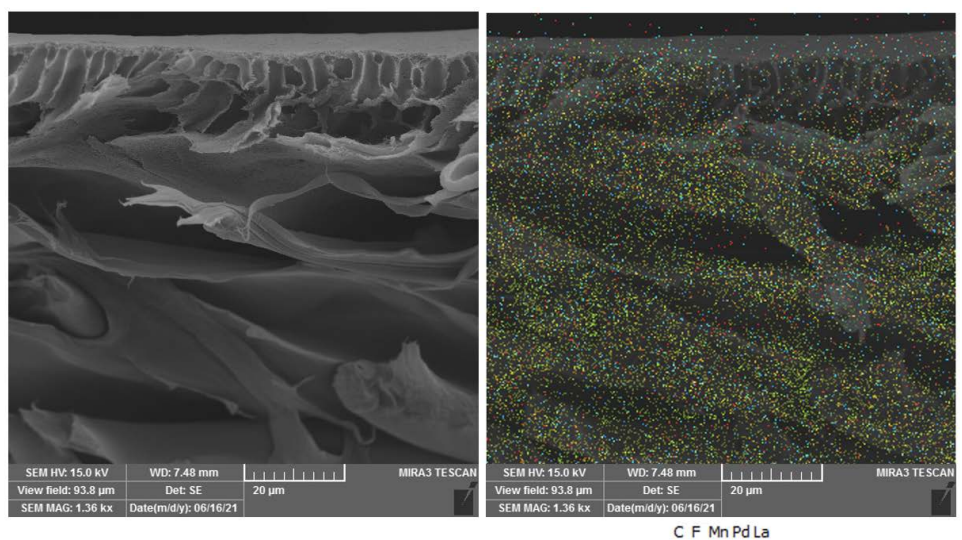


Fig. 3. Energy-dispersive X-ray spectroscopy-mapping of M2-2.

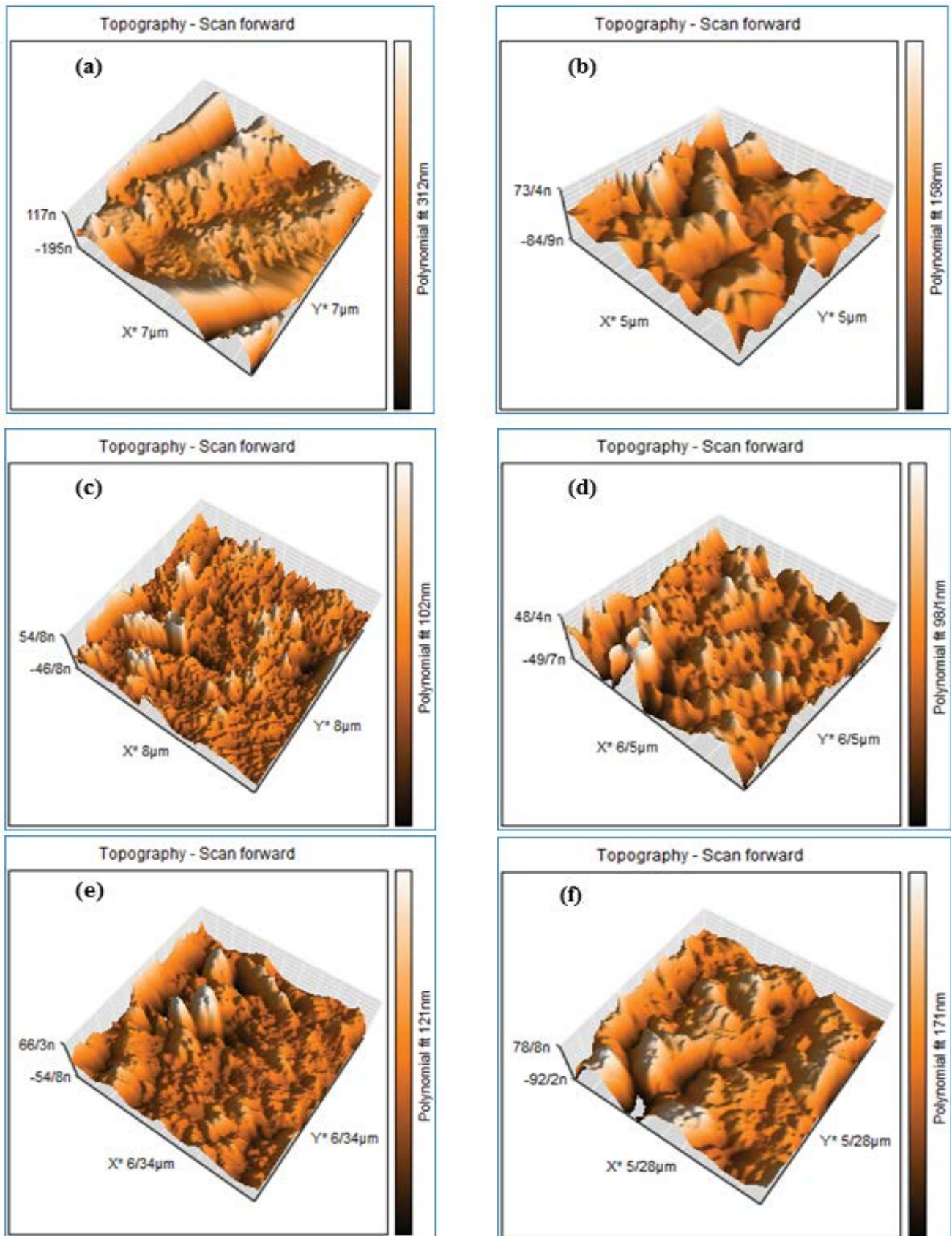


Fig. 4. Three-dimensional atomic force microscopy images of (a) M1, (b) M2, (c) M1-1, (d) M2-1, (e) M1-2, and (f) M2-2.

nanocomposite membranes. As shown in Fig. 5b, the nanocomposite membranes containing Pd-treated nanoparticles had the highest values of porosity, which can be related to the pore formation mechanism. The interfacial stress between polymer and nanoparticles induced by polymer shrinkage during the phase inversion process is released by pore formation [29].

3.4. Pure water flux, antifouling performance, and rejection

Pure water flux is one of the important parameters of membranes related to the membrane’s porosity and pore sizes [30]. The purified water flux of prepared membranes after 20 min at an operating pressure of 0.5 bar is depicted in Fig. 6a and b. As can be seen, the pure water flux of neat PVDF is higher than neat PS. Adding perovskite nanoparticles to the membrane matrix improves the membranes’ hydrophilic nature and porosity, so the pure water flux of nanocomposite membranes is higher than neat membranes. Also, the pure water flux of nanocomposite membranes containing Pd-modified perovskite is higher than other membranes, which may be related to higher porosity and larger inner macropores confirmed by SEM images of the cross-section of membranes. By comparing Fig. 6a and b, it can be concluded that permeate flux of the neat PVDF membrane is higher than the neat PS membrane after 45 min filtration processes. In addition, the modification of neat membranes with perovskite nanoparticles and Pd-modified perovskite nanoparticles

enhances permeation flux which may be related to bigger surface pore size, higher porosity, and hydrophilicity enhancement [29]. The lower permeate flux compared to pure water flux can be associated with the accumulation of humic acid on the membrane’s surface, leading to the concentration polarization effect, pore blocking, and cake formation [26]. The pure water flux of cleaned membranes is lower than the initial pure water flux of membranes related to some irreversible fouling that is not cleaned

Table 1
Parameters of surface roughness of prepared membranes

Membrane ID	Parameters of surface roughness		
	S_a (nm)	S_q (nm)	S_y (nm)
M1	32.606	44.172	432
M2	25.24	12.705	91.95
M1-1	11.37	15.869	166.73
M2-1	12.57	17.47	180.67
M1-2	12.536	17.181	135.26
M2-2	20.849	27.607	206.51

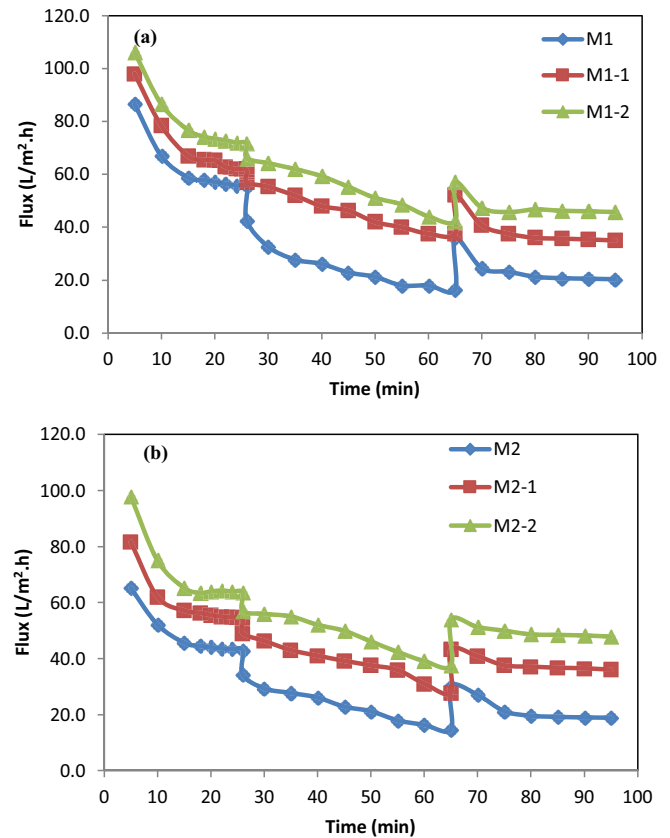


Fig. 6. Time-dependent flux variation of the (a) M1 and modified membranes (b) M2 and modified membranes using humic acid as a pollutant.

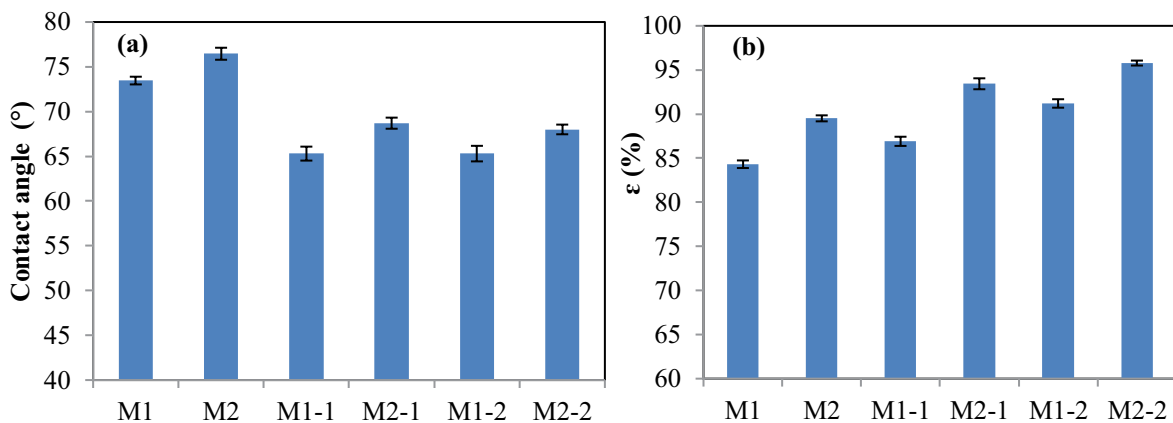


Fig. 5. (a) Contact angle and (b) porosity of neat and nanocomposite membranes.

Table 2
Fouling parameters and rejection of prepared membranes

Membranes	FRR (%)	RFR (%)	IFR (%)	TFR (%)	Rejection (%)
M1	44	9	56	65	79.77
M2	44	11	56	67	57.71
M1-1	62	14	38	52	88.89
M2-1	66	17	34	51	76.89
M1-2	84	23	16	39	91.82
M2-2	88	30	12	42	82.1

during washing membranes. Weak and physical interactions between foulants and membrane surface form reversible fouling. It can be removed by water rinsing, whereas irreversible fouling occurs by strong binding between foulants and membrane surface and pores, leading to membrane damage. Fouling parameters include the FRR, RFR, IFR, and the TFR and rejection are summarized in Table 2. FRR is calculated to evaluate the antifouling performance of prepared membranes. FRR of nanocomposite membranes containing Pd-modified perovskite nanoparticles is highest among other membranes, so they show strong resistance to membrane fouling. FRR of nanocomposite membranes is higher than neat membranes, which can be related to increased hydrophilicity and improved membrane surface smoothness by incorporating perovskite nanoparticles based on contact angle and AFM analysis, respectively. As can be seen, the IFR of membranes is significantly decreased by incorporating perovskite nanoparticles due to the restricted attachment of hydrophobic HA to the membrane surface. Besides high permeate flux, modified membranes indicate higher rejection than neat membranes, which can be related to the lower affinity of hydrophobic HA molecules to interact with hydrophilic membranes.

4. Conclusions

In the current study, novel PVDF and PS nanocomposite membranes containing perovskite nanoparticles are fabricated using the phase inversion method to remove humic acid from contaminated water. The results of AFM analysis confirm higher smoothness of nanocomposite membranes compared with neat PVDF and PS membranes. The prepared membranes' hydrophilicity and pure water flux are improved by incorporating perovskite nanoparticles into the membrane matrix. Investigation of antifouling properties showed that IFR is significantly decreased by embedding perovskite nanoparticles. The results of this study confirmed that perovskite nanoparticles can be used as potential antifouling additives for the fabrication of nanocomposite membranes.

References

- [1] H. Mittal, A. Al Alili, P.P. Morajkar, S.M. Alhassan, GO crosslinked hydrogel nanocomposites of chitosan/carboxymethyl cellulose – a versatile adsorbent for the treatment of dyes contaminated wastewater, *Int. J. Biol. Macromol.*, 167 (2021) 1248–1261.
- [2] P. Mohammadzadeh Pakdel, S.J. Peighambari, N. Arsalani, H. Aghdasinia, Safranin-O cationic dye removal from wastewater using carboxymethyl cellulose-grafted-poly(acrylic acid-co-itaconic acid) nanocomposite hydrogel, *Environ. Res.*, 212 (2022) 113201, doi: 10.1016/j.envres.2022.113201.
- [3] B. Senthil Rathi, P. Senthil Kumar, R. Ponprasath, K. Rohan, N. Jahnavi, An effective separation of toxic arsenic from aquatic environment using electrochemical ion exchange process, *J. Hazard. Mater.*, 412 (2021) 125240, doi: 10.1016/j.jhazmat.2021.125240.
- [4] C. Zhao, J. Zhou, Y. Yan, L. Yang, G. Xing, H. Li, P. Wu, M. Wang, H. Zheng, Application of coagulation/flocculation in oily wastewater treatment: a review, *Sci. Total Environ.*, 765 (2021) 142795, doi: 10.1016/j.scitotenv.2020.142795.
- [5] Y. Xu, Z. Li, K. Su, T. Fan, L. Cao, Mussel-inspired modification of PPS membrane to separate and remove the dyes from the wastewater, *Chem. Eng. J.*, 341 (2018) 371–382.
- [6] E. Derakhshani, A. Naghizadeh, Optimization of humic acid removal by adsorption onto bentonite and montmorillonite nanoparticles, *J. Mol. Liq.*, 259 (2018) 76–81.
- [7] H. Namdar, A. Akbari, R. Yegani, H. Roghani-Mamaqani, Influence of aspartic acid functionalized graphene oxide presence in polyvinylchloride mixed matrix membranes on chromium removal from aqueous feed containing humic acid, *J. Environ. Chem. Eng.*, 9 (2021) 104685, doi: 10.1016/j.jece.2020.104685.
- [8] J. Lowe, Md.M. Hossain, Application of ultrafiltration membranes for removal of humic acid from drinking water, *Desalination*, 218 (2008) 343–354.
- [9] P. Jarvis, I. Carra, M. Jafari, S.J. Judd, Ceramic vs polymeric membrane implementation for potable water treatment, *Water Res.*, 215 (2022) 118269, doi: 10.1016/j.watres.2022.118269.
- [10] S. Khakpour, Y. Jafarzadeh, R. Yegani, Incorporation of graphene oxide/nanodiamond nanocomposite into PVC ultrafiltration membranes, *Chem. Eng. Res. Des.*, 152 (2019) 60–70.
- [11] H. Etemadi, M. Fonouni, R. Yegani, Investigation of antifouling properties of polypropylene/TiO₂ nanocomposite membrane under different aeration rate in membrane bioreactor system, *Biotechnol. Rep.*, 25 (2020) e00414, doi: 10.1016/j.btre.2019.e00414.
- [12] I.V. Maggay, M.-L. Yu, D.-M. Wang, C.-H. Chiang, Y. Chang, A. Venault, Strategy to prepare skin-free and macrovoid-free polysulfone membranes via the NIPS process, *J. Membr. Sci.*, 655 (2022) 120597, doi: 10.1016/j.memsci.2022.120597.
- [13] M. Homayoonfal, M.R. Mehrnia, S. Rahmani, Y. Mohades Mojtahedi, Fabrication of alumina/polysulfone nanocomposite membranes with biofouling mitigation approach in membrane bioreactors, *J. Ind. Eng. Chem.*, 22 (2015) 357–367.
- [14] J.-H. Jiang, L.-P. Zhu, H.-T. Zhang, B.-K. Zhu, Y.-Y. Xu, Improved hydrodynamic permeability and antifouling properties of poly(vinylidene fluoride) membranes using polydopamine nanoparticles as additives, *J. Membr. Sci.*, 457 (2014) 73–81.
- [15] M. Amini, H. Etemadi, A. Akbarzadeh, R. Yegani, Preparation and performance evaluation of high-density polyethylene/silica nanocomposite membranes in membrane bioreactor system, *Biochem. Eng. J.*, 127 (2017) 196–205.
- [16] F. Beygmohammadi, H. Nourizadeh Kazerouni, Y. Jafarzadeh, H. Hazrati, R. Yegani, Preparation and characterization of PVDF/PVP-GO membranes to be used in MBR system, *Chem. Eng. Res. Des.*, 154 (2020) 232–240.
- [17] S. Abd Hamid, M. Shahadat, B. Ballinger, S. Farhan Azha, S. Ismail, S. Wazed Ali, S. Ziauddin Ahammad, Role of clay-based membrane for removal of copper from aqueous solution, *J. Saudi Chem. Soc.*, 24 (2020) 785–798.
- [18] G. Tian, Z. Huang, H. Wang, C. Cui, Y. Zhang, Polycaprolactone nanofiber membrane modified with halloysite and ZnO for anti-bacterial and air filtration, *Appl. Clay Sci.*, 223 (2022) 106512, doi: 10.1016/j.clay.2022.106512.
- [19] M. Ahsani, H. Hazrati, M. Javadi, M. Ulbricht, R. Yegani, Preparation of antibiofouling nanocomposite PVDF/Ag-SiO₂ membrane and long-term performance evaluation in the MBR system fed by real pharmaceutical wastewater, *Sep. Purif. Technol.*, 249 (2020) 116938, doi: 10.1016/j.seppur.2020.116938.

- [20] B. Eryildiz, B. Ozbey-Unal, E. Gezmis-Yavuz, D.Y. Koseoglu-Imer, B. Keskinler, I. Koyuncu, Flux-enhanced reduced graphene oxide (rGO)/PVDF nanofibrous membrane distillation membranes for the removal of boron from geothermal water, *Sep. Purif. Technol.*, 274 (2021) 119058, doi: 10.1016/j.seppur.2021.119058.
- [21] V. Vatanpour, H. Karimi, S. Imanian Ghazanlou, Y. Mansourpanah, M.R. Ganjali, A. Badiei, E. Pourbashir, M.R. Saeb, Anti-fouling polyethersulfone nanofiltration membranes aided by amine-functionalized boron nitride nanosheets with improved separation performance, *J. Environ. Chem. Eng.*, 8 (2020) 104454, doi: 10.1016/j.jece.2020.104454.
- [22] Y. Mansourpanah, H. Soltani Afarani, K. Alizadeh, M. Tabatabaei, Enhancing the performance and antifouling properties of nanoporous PES membranes using microwave-assisted grafting of chitosan, *Desalination*, 322 (2013) 60–68.
- [23] N. Nasrollahi, S. Aber, V. Vatanpour, N.M. Mahmoodi, Development of hydrophilic microporous PES ultrafiltration membrane containing CuO nanoparticles with improved antifouling and separation performance, *Mater. Chem. Phys.*, 222 (2019) 338–350.
- [24] T.Q.N. Tran, S.W. Yoon, B.J. Park, H.H. Yoon, CeO₂-modified LaNi_{0.6}Fe_{0.4}O₃ perovskite and MWCNT nanocomposite for electrocatalytic oxidation and detection of urea, *J. Electroanal. Chem.*, 818 (2018) 76–83.
- [25] A. Tarjomannejad, A. Niaei, A. Farzi, D. Salari, P. Rashidi Zonouz, Catalytic oxidation of CO over LaMn_{1-x}B_xO₃ (B = Cu, Fe) perovskite-type oxides, *Catal. Lett.*, 146 (2016) 1544–1551.
- [26] E. Shokri, E. Shahed, M. Hermani, H. Etemadi, Towards enhanced fouling resistance of PVC ultrafiltration membrane using modified montmorillonite with folic acid, *Appl. Clay Sci.*, 200 (2021) 105906, doi: 10.1016/j.clay.2020.105906.
- [27] M. Safarpour, A. Khataee, V. Vatanpour, Preparation of a novel polyvinylidene fluoride (PVDF) ultrafiltration membrane modified with reduced graphene oxide/titanium dioxide (TiO₂) nanocomposite with enhanced hydrophilicity and antifouling properties, *Ind. Eng. Chem. Res.*, 53 (2014) 13370–13382.
- [28] P. Salimi, A. Aroujalian, D. Iranshahi, Graft copolymerization of zwitterionic monomer on the polyethersulfone membrane surface by corona air plasma for separation of oily wastewater, *Sep. Purif. Technol.*, 258 (2021) 117939, doi: 10.1016/j.seppur.2020.117939.
- [29] H. Etemadi, H. Qazvini, Investigation of alumina nanoparticles role on the critical flux and performance of polyvinyl chloride membrane in a submerged membrane system for the removal of humic acid, *Polym. Bull.*, 78 (2021) 2645–2662.
- [30] T. Rajasekhar, M. Trinadh, P. Veera Babu, A.V. Sesha Sainath, A.V.R. Reddy, Oil-water emulsion separation using ultrafiltration membranes based on novel blends of poly(vinylidene fluoride) and amphiphilic tri-block copolymer containing carboxylic acid functional group, *J. Membr. Sci.*, 481 (2015) 82–93.